JOURNAL OF CATALYSIS 72, 139–148 (1981)

Infrared and Raman Studies of Amorphous MoS_3 and Poorly Crystalline MoS_2

C. H. CHANG[1] AND S. S. CHAN

Corporate Research-Science Laboratories, Exxon Research and Engineering Company, Linden, New Jersey 07036

Received March 24, 1981; revised July 21, 1981

Amorphous MoS_3 and poorly crystalline MoS_2 have been studied using infrared and Raman spectroscopies. While poorly crystalline MoS_2 exhibits sharp infrared bands at 385 and 470 cm^{-1}, broad bands at 287, 335, 373, and 522 cm^{-1} were observed for the amorphous MoS_3. In contrast to poorly crystalline MoS_2 where sharp Raman peaks were measured at 384 and 408 cm^{-1}, the Raman spectrum of amorphous MoS_3 showed broad peaks at 215, 317, 431, and 528 cm^{-1}. The band profiles of both the ir and Raman spectra of the MoS_3 sample indicate the amorphous nature of the material. This is consistent with results obtained by other techniques. The comparison of the Raman spectrum of MoS_3 and that of amorphous MoS_2 reported in the literature indicates that local bondings in these materials are dissimilar. The presence of broad bands at 522 cm^{-1} in ir and 528 cm^{-1} in Raman spectra of MoS_3 is evidence for polysulfide bonds indicated by the XPS spectrum of the material. These results support a chain-like structural model for amorphous MoS_3 similar to that for crystalline MS_3 (M = Ti, Zr, Hf, Nb, Ta, and U). The thermal stability of MoS_3 and the effect of laser power on the Raman spectrum of MoS_3 were also studied.

1. INTRODUCTION

In recent years considerable interest has been shown on molybdenum sulfides because they are widely used as solid lubricants and as catalysts in hydrodesulfurization and hydrotreating processes. Furthermore, these compounds have been found to show interesting electrochemical properties as cathode materials in ambient secondary alkali metal cells (*1*, *2*). Several sulfides of molybdenum have been reported: MoS_4, MoS_3, Mo_2S_5, MoS_2, and Mo_2S_3 (*3*, *4*). MoS_2 and MoS_3 have received most of the attention because of their stability and interesting properties.

Molybdenum trisulfide can be easily prepared by precipitation from an acidic aqueous solution of ammonium paramolybdate with H_2S (*5*) or thermal decomposition of ammonium tetrathiomolybdate (*3*). The MoS_3 sample thus prepared is amorphous to X rays. Earlier structural studies of the material provided no conclusive evidence that MoS_3 is a definite chemical compound rather than an intimate mixture of subcrystalline MoS_2 and amorphous sulfur (*6*, *7*). Stevens and Edmonds measured X-ray photoelectron spectra (XPS) of molybdenum sulfides and concluded that MoS_3 is an intimate association of subcrystallline MoS_2 and amorphous sulfur (*8*).

Most recently, Diemann (*9*) reinvestigated the structure of MoS_3 and its related noncrystalline trichalcogenides (WS_3 and $MoSe_3$). He concluded that these trichalcogenides are compounds in their own right, and not a mixture as suggested by earlier investigators (*6*–*8*). Liang and his coworkers studied the detailed structures and physical properties of MoS_3 and WS_3 using high-resolution X-ray radial distribution analysis (RDF), magnetic susceptibility measurements, XPS, extended X-ray absorption fine structure (EXAFS), and vibrational spectroscopies (*10*, *11*). The experimental results showed the dimerization of metal atoms and the presence of polysulfide bonds. A chain-like structure analogous to that of the crystalline trichalcogenides of

---

[1] To whom correspondence should be addressed.

0021-9517/81/110139-10$02.00/0

the neighboring IVB and VB elements (Ti, Zr, Hf, V, Nb, Ta) was proposed for amorphous MS_3. In this structural model, adjacent metal atoms are bridged with three sulfur atoms along the chain. The structure has every two metal atoms in the chain paired up with a shorter metal–metal distance and one polysulfide bond in every other sulfur triangle. This constitutes a formal charge state of $M^{V}(S_2{}^{2-})_{1/2}\,(S^{2-})_2$ for the amorphous trichalcogenides.

Infrared and Raman studies of MoS_3 were first reported by Stevens and Edmonds in an attempt to detect polysulfide bonds (*8*). However, Raman bands associated with S–S stretching vibrations were not observed. Instead, well-defined bands were observed in the region 100–450 cm^{-1}. This is in contrast to the broad and uncharacteristic bands observed in the ir spectrum of WS_3 (*9*) and the Raman spectrum of amorphous MoS_2 (*12*) reported in the literature.

In view of the possible existence of MoS_3 on the surface of sulfided CoMo catalysts (*13*) and the renewed interest in the structure of the amorphous trichalcogenides, we studied the vibrational spectra of these trichalcogenides. Some results have been summarized in a previous publication (*11*). Complete results of our infrared and Raman studies of amorphous molybdenum trisulfide and poorly crystalline MoS_2 are presented in this paper.

2. EXPERIMENTAL METHODS

a. Sample Preparation

The MoS_3 sample used in the present study was prepared by the thermal decomposition of ammonium tetrathiomolybdate, $(NH_4)_2MoS_4$. The thiomolybdate was prepared at ambient temperature by passing H_2S through the ammonium hydroxide solution of ammonium paramolybdate, $(NH_4)_6Mo_7O_{24} \cdot 4H_2O$ (Alfa Products) (*14*). Fine crystals of $(NH_4)_2MoS_4$ were collected and washed with methanol. After drying under vacuum, the $(NH_4)_2MoS_4$ sample was analyzed by X-ray diffractometry (XRD) and Fourier transform-infrared absorption spectroscopy (FT-ir). The absence of absorption bands in the region 800–1100 cm^{-1} indicated that the sample was free of oxygen impurities.

For the preparation of MoS_3, $(NH_4)_2MoS_4$ was heated in oxygen-free inert gas (He) at 200°C for a period of 2 days. Analysis of the final product showed a S : Mo ratio of close to 3. In order to compare the vibrational spectra of MoS_3 with those of MoO_3 and subcrystalline MoS_2, samples of crystalline MoO_3 and poorly crystalline MoS_2 were also prepared.

MoO_3 was prepared by the thermal decomposition of $(NH_4)_6Mo_7O_{24} \cdot 4H_2O$ in dry and oxygen-free N_2 at 250°C. Poorly crystalline MoS_2 samples were prepared by the thermal decomposition of $(NH_4)_2MoS_4$ in H_2S at 350 and 400°C, respectively, to ensure minimum oxygen contaminations in the products. All samples were stored in a helium dry box before they were studied.

Elemental analyses of molybdenum sulfides were carried out using a combustion-gas chromatographic method. Samples of about 20 mg were burned in a stream of O_2 and the SO_2 produced was analyzed by a dual-column gas chromatograph using the same O_2 stream as a carrier gas. Predried sulfur flowers (Allied Chemical) were used to calibrate the combustion-gas chromatographic system. A linear correlation between the total integrated counts for SO_2 signals from the gas chromatograph and weights of sulfur was established and used as a calibration curve. The combustion temperature is controlled as low as possible. The combustion residues of MoO_3 are accurately weighed and the Mo content of molybdenum sulfides is thus determined. Excellent agreements with results from conventional methods (Galbraith Laboratories, Inc.) were obtained for some samples.

b. Instrumentation

Infrared absorption spectra were obtained with a Fourier transform-infrared spectrometer manufactured by Digilab Inc. The FT-ir spectra were taken either on KBr or CsI pellets depending on the ir frequency range. These pellets contained typically 0.5 to 1.0 wt% of the material being studied. In the far-ir region, a 12.5-μm Mylar beamsplitter was used. All spectra were composites of 500 individual scans and all were taken at room temperature with an instrumental resolution of 4.0 cm^{-1}.

Raman spectra were recorded on a Spex Ramalog (14018) equipped with a triple monochromator and a cooled RCA GaAs photomultiplier. Room-temperature Raman spectra were taken in the backscattering geometry. These measurements were carried out employing laser excitations with the Ar$^+$ 514.5-nm line (Spectra Physics model 165). A laser filter monochromator (Anaspec 300-S) with 0.4-nm bandwidth was used to filter out plasma lines. Raman spectra were obtained using sample powders pressed on a KBr disk. The sample disk was rotated at a speed of about 1500 rpm to minimize sample heating and/or degradation. However, the laser power was varied to study the effect of laser intensity on the MoS_3 sample. All Raman spectra were recorded with a spectral resolution of 2 cm^{-1} and a scan rate of 0.2 cm^{-1}/sec. Photo-counting detection with a time constant of 10 sec was used throughout this investigation.

Before samples were studied for their vibrational spectra, X-ray diffraction patterns were obtained on powder samples using an X-ray diffractometer manufactured by Philips Electronic Instruments. All patterns were taken with Cu*Kα* radiation.

3. EXPERIMENTAL RESULTS

In Fig. 1, the infrared absorption spectrum of MoS_3 in the region 100–550 cm^{-1} (CsI pellet) is shown along with the spectra of elemental sulfur and a poorly crystalline MoS_2 prepared by the thermal decomposition of $(NH_4)_2MoS_4$ at 350°C. For MoS_3 two broad bands at 520 and 545 cm^{-1} are distinguishable above a sloping background absorption. No additional band was observed for MoS_3 in the ir region 450–4000 cm^{-1} (KBr pellet).

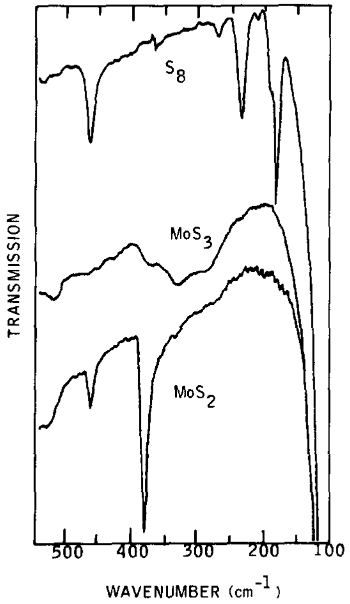

FIG. 1. Fourier transform-infrared spectra of amorphous MoS_3, poorly crystalline MoS_2, and elemental sulfur.

In order to compare the FT-ir spectrum of MoS_3 with those of subcrystalline MoS_2, FT-ir spectra of poorly crystalline MoS_2 were taken and are shown in Fig. 2. The crystallinity of the MoS_2 sample is indicated by the XRD pattern as shown in Fig. 3 along with that of MoS_3.

The Raman spectrum of MoS_3 is shown in Fig. 4. This spectrum was recorded with a laser power of approximately 12 mW measured at the sample. As the laser power was increased, new and well-defined Raman bands were recorded as shown in Fig. 5. The positions of these bands are given in Table 1 where Raman band positions for crystalline MoS_2 and MoO_3 obtained in this study are also listed.

The Raman spectrum of MoS_3 shows broad and weak bands owing to the low laser power and to the amorphous nature of the material. Amorphous MoS_2 prepared by rf sputtering of polycrystalline MoS_2 onto glass slides also shows broad and weak Ra-

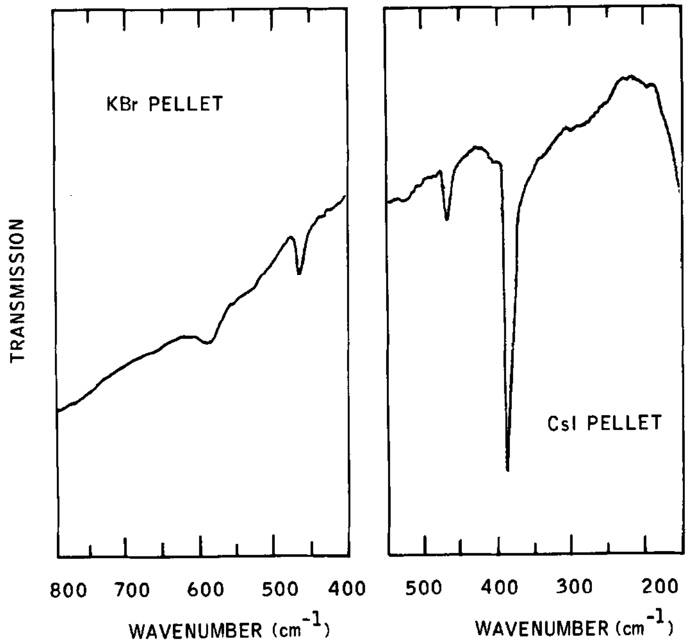

FIG. 2. Fourier transform-infrared spectra of poorly crystalline MoS_2 prepared at 400°C.

man bands (12). The vertical tick marks in Fig. 4 are the result of photo-counting detection with a time constant of 10 sec and a scan rate of 0.2 cm^{-1}/sec. The spectrum changes slightly even at a laser power of 12 mW if the measurement is repeated on the same spot of the sample. However, by recording the Raman spectrum at different spots of the sample, the vibrational spectrum of MoS_3 was reproduced several times at 12 mW. The spectra taken at higher laser powers changed depending on the duration of laser illumination. It appears that different chemical species were formed during the Raman measurements at the higher powers.

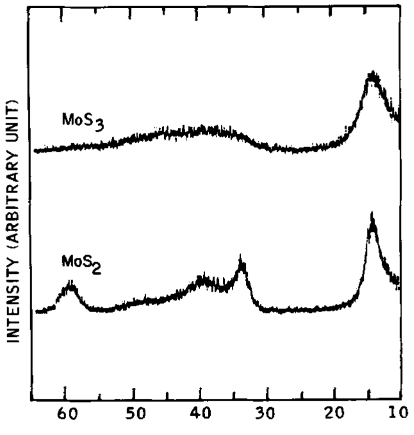

FIG. 3. X-Ray diffraction patterns of amorphous MoS_3 and poorly crystalline MoS_2 prepared at 400°C.

In order to identify the chemical species formed during the laser excitation of MoS_3, a Raman spectrum of MoO_3 was also obtained under similar experimental conditions as shown in Fig. 6. The crystalline MoO_3 and MoS_2 samples were prepared by the thermal decomposition of $(NH_4)_6Mo_7O_{24} \cdot 4H_2O$ and $(NH_4)_2MoS_4$, respectively, in an inert atmosphere.

4. DISCUSSION OF RESULTS

Despite the widespread use of the active sulfided Co–Mo catalysts in hydrotreating processes, fundamental studies on this chemical system have largely been limited to their precursors, Co–Mo oxides. The lack of fundamental information on the sulfided catalyst is partly due to the difficulty in obtaining good data on sulfides.

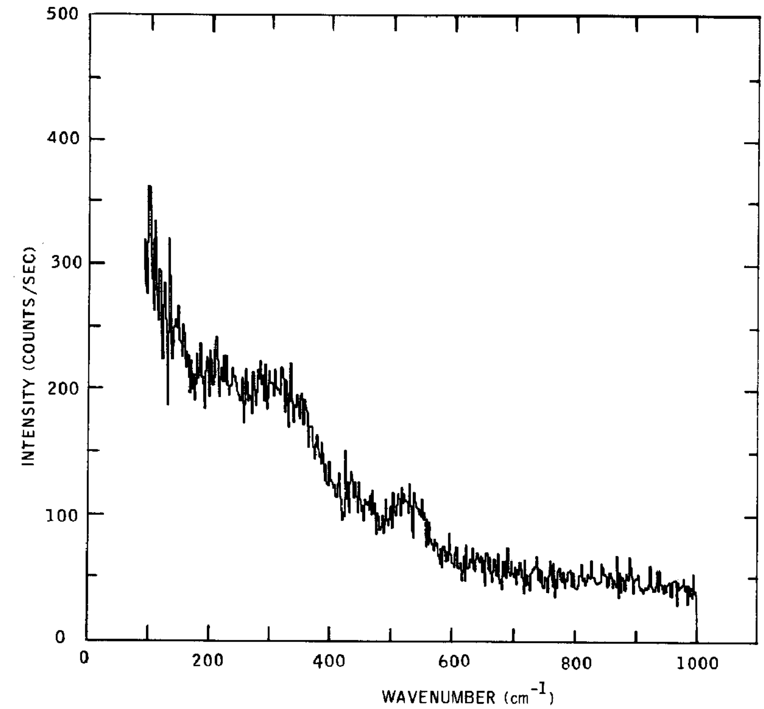

FIG. 4. Raman spectrum of amorphous MoS_3.

MoS_3 is a typical example. While the poorly crystalline MoS_2 exhibits sharp FT-ir absorption bands at 385 and 470 cm^{-1} (Fig. 1), which are characteristic of hexagonal MoS_2 (*15*, *16*), broad and weak bands in the absorption profile of MoS_3 indicate the amorphous nature of the material. This is consistent with the X-ray diffraction pattern of the MoS_3 (*3*, *7*).

The FT-ir spectrum of MoS_3 is similar to that of WS_3 reported by Diemann in the region 70–400 cm^{-1} (*9*). However, it bears no resemblance to those of S_8 (Fig. 1) and other sulfur allotropes (*17*). This result indicates that there is no significant amount of excess sulfur in the MoS_3 sample studied.

Although the thermal decomposition of MoS_3 and the structural evolution of MoS_2 from MoS_3 have been extensively investigated (*3*, *7*, *18*), the effect of the short-range order around the molybdenum and sulfur atoms on the vibrational spectrum of MoS_2 has not been reported. The structural evolution of MoS_2 during the thermal de-

TABLE 1

Raman Spectra of MoS_3 Recorded with Different Laser Powers (cm^{-1})

MoS_3			MoS_2	MoO_3	
12 mW	25 mW	40 mW	50 mW	12 mW	60 mW[a]
		109[b]		84	
		120		102	
		130		120	117
		160		130	129
				160	158
				198	199
215	202	201[b]			
	225	225		225	218
				245	247
	273	285[b]		292	284, 292
317					
	352	353[b]		338	337
				365	367
	382	382	384	380	380
	408	407	408		
431	461	459		465	
	493	492[b]			
528	565	566[b]			
	660	663		666	667
	734	733[b]			
	820	820		821	820
	995	994		996	996

[a] Data taken from Jeziorowski, H., Knozinger, H., Grange, P., and Gajardo, P., *J. Phys. Chem.* **84**, 1825 (1980).

[b] Bands not identified.

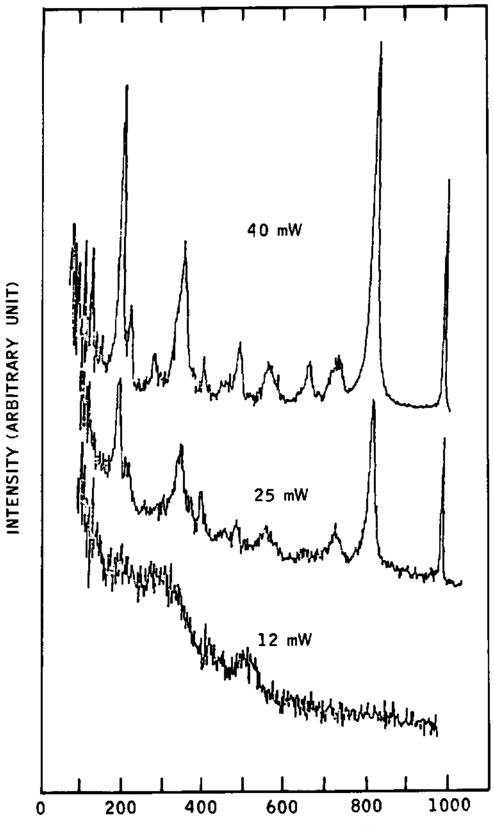

FIG. 5. Raman spectra of MoS_3 at various laser powers.

composition of $(NH_4)_2MoS_4$ in an oxygen-free atmosphere is being studied. However, it has been reported that as the decomposition temperature was increased, the crystallite size of the molybdenum sulfide increased as estimated from X-ray line broadening (*18, 19*). Table 2 gives the sulfur-to-metal ratio of poorly crystalline MoS_2 prepared at 400°C. The sulfur-to-metal ratio is in agreement with earlier results (*3, 20*). While the intensities of FT-ir bands of the poorly crystalline MoS_2 in the region 150–500 cm^{-1} (Fig. 2) are similar to those of hexagonal MoS_2 crystals (*15, 16*), the poorly crystalline MoS_2 samples, which contain sulfur-to-metal ratios higher than 2, show an ir band at about 585 cm^{-1} (Fig. 2). In contrast, the FT-ir spectrum of MoS_3 contains no significant common features to those of poorly crystalline MoS_2. These results indicate that the short-range order of MoS_3 around the molybdenum and sulfur atoms is quite different from that of hexagonal MoS_2. They support the conclusion that MoS_3 is a unique chemical compound in agreement with previous investigators (*9–11*).

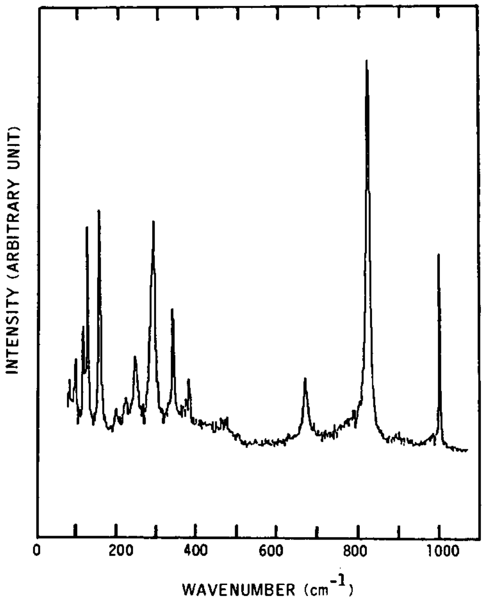

FIG. 6. Raman spectra of crystalline MoO_3.

The band profile of the Raman spectrum of MoS_3 (Fig. 4) in comparison with those of poorly crystalline MoS_2 and crystalline MoO_3 (Fig. 6), also suggests the amorphous nature of the material. Furthermore, the

TABLE 2

The S/Mo Ratio of Poorly Crystalline Molybdenum Sulfides

Preparation temperature (°C)	S/Mo ratio		
	This work	Rode–Lebedev[a]	Wildervanck–Jellinek[b]
350		2.43	2.40
400	2.38	—	

[a] See Ref. (*20*).
[b] See Ref. (*3*).

TABLE 3

Bond Distances and Vibrational Frequencies in Molybdenum–Sulfur Compounds

Compound	Mo–S (Å)	$\nu_{Mo-S}{}^{a}$ (cm^{-1})	S–S (Å)	ν_{S-S} (cm^{-1})
$MoO_2S_2{}^{2-}$	2.19^{b}	484^{c}	—	—
$MoS_4{}^{2-}$	2.17^{d}	478^{c}	—	—
MoS_2	2.36^{e}	385^{c}	—	—
$(Mo_2O_2S_2(S_2)_2)^{2-}$	2.38, 2.44^{f}	359^{c}	2.07–2.09^{f}	510 (ir)^{c,g} 515 (Raman)^{g}
$(Mo_2(S_2)_6)^{2-}$	2.38, 2.45^{h}	340^{h}	2.04–2.06^{h}	530 (ir)^{h}
MoS_3	2.39^{e} 2.41^{i}	335^{c}		522 (ir)^{c} 528 (Raman)^{c}

[a] All ir bands.

[b] Kutzler, F. W., Scott, R. A., Berg, J. M., Hodgson, K. O., Doniach, S., Cramer, S. P., and Chang, C. H., to be published.

[c] This work.

[d] Schafer, H., Schafer, G., and Weiss, A., *Z. Naturforsch. B* **19**, 76 (1964).

[e] See Ref. (*7*).

[f] Clegg, W., Mohan, N., Muller, A., Neumann, A., Rittner, W., and Sheldrick, G. M., *Inorg. Chem.* **19**, 2066 (1980).

[g] See Ref. (*22*).

[h] See Ref. (*23*).

[i] See Ref. (*11*).

comparison of the Raman spectrum of MoS_3 with that of thin films of amorphous MoS_2 reported by Lannin (*12*) indicates that local bondings in these materials are dissimilar. In addition, no Raman bands associated with S_8 and disordered sulfur (*21*) were observed in the Raman spectrum of MoS_3.

Although the features of both the FT-ir and Raman spectra for MoS_3 are broad, band centers can be determined. The ir of MoS_3 (see Fig. 1), shows four bands at 287, 335, 373, and 522 cm^{-1}, while bands at 215, 317, 431, and 528 cm^{-1} are observed in Raman (see Table 1). The dominant band at 335 cm^{-1} in ir and 317 cm^{-1} in Raman is probably associated with the Mo–S stretching frequency. As the Mo–S bond distance increases the stretching frequency, ν_{Mo-S}, decreases as shown in Table 3. The assignment of the 335-cm^{-1} ir band as the Mo–S stretching mode suggests a Mo–S distance of about 2.4 Å which is consistent with the results obtained with RDF (2.39 Å) (*7*) and EXAFS (2.41 Å) (*11*).

The presence of broad bands at 522 cm^{-1} in FT-ir and 528 cm^{-1} in Raman spectra of the MoS_3 sample suggests the existence of polysulfide bonds as indicated by the XPS spectrum of the material (*8*, *10*). Similar S–S stretching frequencies of 510 (ir) and 515 cm^{-1} (Raman) have been observed for the tetramethylammonium salt of $(Mo_2O_2S_2(S_2)_2)^{2-}$ (*22*). A S–S stretching frequency of 530 cm^{-1} (ir) has been observed for $(NH_4)_2((S_2)_2Mo(S_2)_2Mo(S_2)_2)$ (*23*) and $Cs_2(MoO(S_2)_2(COS{-}COO))$ (*24*) as well. The close resemblance of the S–S frequency of MoS_3 for the polysulfide bonds to that in the molybdenum–sulfur compounds containing η-disulfido groups suggests that the S–S bond length in MoS_3 is about 2.05 Å (see Table 3).

Recently, ir and Raman spectra of structurally related transition-metal trisulfides (M = Ti, Zr, Hf, Nb, Ta, U) have been

TABLE 4

Vibrational Spectra of the Linear-Chain Trisulfides at 300 K (cm^{-1})

TiS_3		ZrS_3		HfS_3		NbS_3	TaS_3	US_3
ir[a]	R[b]	ir[a]	R[c]	ir[d]	R[e]	ir[a]	R[f]	ir[a]
560(w)	562(m)	529(w)	530(vs)	548(w)	527(w)	570(w)	496(m)	505(w)
400(w)	375(vs)	365(w)		352(m)	322(vs)	400(w)	405(w)	288(w)
	366(w)		320(s)	343(vw)				
355(m)	304(s)	315(s)		278(s)	275(m)	342(vs)	370(w)	260(vs)
	297		282(vs)		262(s)	332(vs)	338(m)	
285(vs)	277(w)	250(vs)	277(s)	240(s)	246(m)	298(w)	283(vs)	210(vs)
						275(vw)		
220(w)		225(vw)		220(w)	221(w)	268(m)	210(vw)	
	178(m)		152(m)		140(w)	258(m)	152(w)	
	136(w)		125(s)		130(vw)	243(s)		
	104(w)							

[a] See Ref. (*29, 30*).
[b] See Ref. (*25*).
[c] See Ref. (*26*).
[d] See Ref. (*30*).
[e] See Ref. (*27*).
[f] See Ref. (*28*).

reported (*25–30*). These compounds are related to the structures of $ZrSe_3$ (*31*) and they can be formulated as $M^{4+}(S_2)^{2-}S^{2-}$ in agreement with XPS spectra (*32*). Perrin and his co-workers have assigned vibrational frequencies for TiS_3, ZrS_3, NbS_3, and US_3 (*29*). As shown in Table 4, the existence of the (S–S) groups in these com-

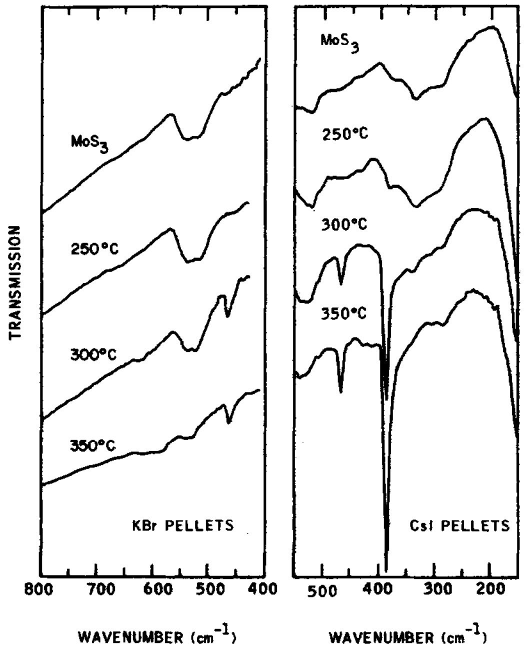

FIG. 7. FT-ir spectra of MoS_3 and the decomposition products of $(NH_4)_2MoS_4$ at 250, 300, and 350°C.

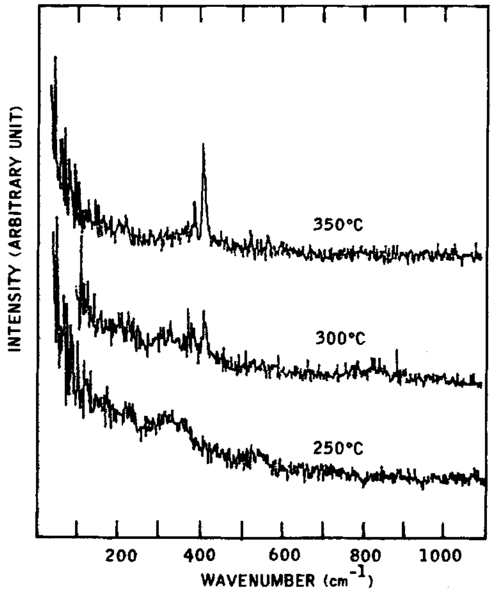

FIG. 8. Raman spectra of the decomposition products of $(NH_4)_2MoS_4$ at 250, 300, and 350°C.

pounds is associated with vibrational bands ranging from 496 cm^{-1} (Raman) for TaS_3 to 562 cm^{-1} (Raman) for TiS_3. This reaffirms the assignment of the 522-cm^{-1} ir band and the 528-cm^{-1} Raman band of MoS_3 as the S–S stretching mode and supports the chain-like model proposed for the structure of amorphous MoS_3 (*10, 11*).

Since FT-ir and Raman spectra of amorphous MoS_3 are distinctively different from those of polycrystalline MoS_2, the vibrational spectroscopy can be used as a sensitive diagnostic probe to study the existence of the amorphous phase. Ammonium thiomolybdate was isothermally decomposed in H_2S for 30 min at temperatures ranging from 250 to 350°C where the thermogram of the material shows a plateau (*11*). FT-ir spectra of these decomposition products and that of MoS_3 are shown in Fig. 7. Raman spectra of the decomposition products are shown in Fig. 8. At 250 and 300°C, the decomposition products contained mainly amorphous MoS_3 after the thermal treatment. However, the ir absorption at 383 cm^{-1} and the Raman band at 408 cm^{-1} suggest the existence of poorly crystalline MoS_2 phase in the 300°C sample. A temperature increase of 50°C to 350°C for half an hour resulted in only a small amount of amorphous MoS_3 in the product (Figs. 7 and 8). A significant amount of poorly crystalline MoS_2 was detected after the ammonium thiomolybdate was heated for more than 20 hr at 250°C. As shown in Fig. 9, the existence of the poorly crystalline MoS_2 can be detected by the XRD peak at 58° and/or by the ir absorption at 470 cm^{-1}. This suggests that the amorphous MoS_3 is stable only up to about 200°C and at 350°C, the phase transition from amorphous MoS_3 to poorly crystalline MoS_2 is kinetically fast. On Co–Mo catalysts, which had experienced a temperature higher than 350°C, the existence of the amorphous MoS_3 is doubtful unless Co and/or the support plays a role in stabilizing the amorphous phase.

Care must be taken to perform Raman investigations of amorphous MoS_3 under low laser power since our studies show that the Raman spectrum of MoS_3 changes with increasing laser power. As shown in Fig. 5, the Raman spectrum of MoS_3, obtained at 12 mW, contains no well-defined peaks. As the laser power at the sample was increased beyond 25 mW, a number of sharp Raman bands were recorded (see Table 1). Comparison of these Raman spectra with those of crystalline MoS_2 and MoO_3 showed that amorphous MoS_3 was decomposed to MoS_2 and also oxidized to MoO_3 under the laser illumination. In addition to Raman bands associated with MoS_2 and MoO_3, bands at

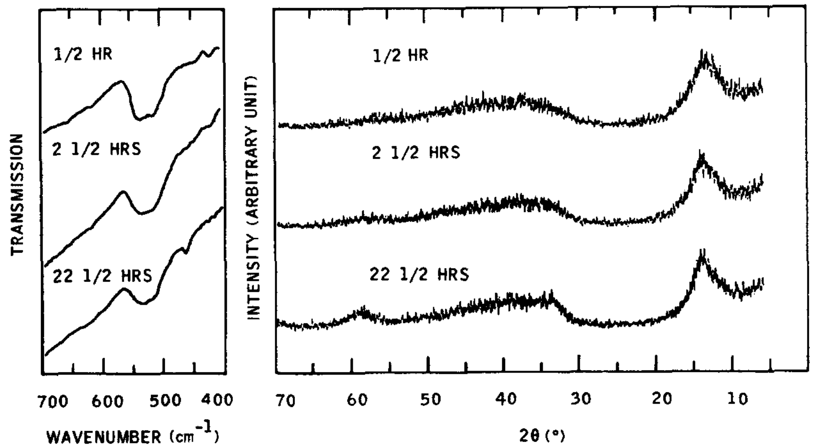

FIG. 9. FT-ir and X-ray diffraction patterns of the decomposition products of $(NH_4)_2MoS_4$ at 250°C for ½, 2½, and 22½ hr.

109(s), 201(vs), 285(w), 353(s), 492(m), 566(m), and 733(m) cm^{-1} were also measured. These Raman bands may be associated with molybdenum–oxygen and/or molybdenum–oxysulfur compounds which exist, at least in transient, with molecular structures different from those of MoS_3 and MoO_3. Raman bands at different frequencies have been observed for molybdates in solutions depending on the state of aggregation of the molybdenum polyanions in the solution (*33*). Weak Raman bands in the region 215(m), 355(m), 570(w), and 735(w) cm^{-1} were observed for γ-alumina- and SiO_2-supported molybdenum oxides prepared from $(NH_4)_6Mo_7O_{24} \cdot 4H_2O$ and dried at 110°C (*33*). Comparison of these molybdate bands to those unidentified Raman frequencies listed above suggests that the molecular species associated with these bands may have structures similar to that of the molybdate. However, the exact identifications of these Raman bands have not been possible and will be the subject of a future study.

ACKNOWLEDGMENTS

The authors wish to express their appreciation to Dr. J. M. Brown for obtaining the Fourier transform infrared spectra used in this study. Special thanks are extended to Drs. R. A. Beyerlein, R. R. Chianelli, and K. S. Liang for valuable discussions.

REFERENCES

1. Jacobson, A. J., Chianelli, R. R., Rich, S. M., and Whittingham, M. S., *Mater. Res. Bull.* **14,** 1437 (1979).
2. Jacobson, A. J., Chianelli,, R. R., and Whittingham, M. S., *J. Electrochem. Soc.* **126,** 2277 (1979).
3. Wildervanck, J. C., and Jellinek, F., *Z. Anorg. Allg. Chem.* **328,** 309 (1964).
4. Tsigdinos, G. A., *Top. Curr. Chem.* **76,** 65 (1978).
5. Moldavski, B. L., *et al., J. Gen. Chem. USSR* **3,** 603 (1933).
6. Hoorhoeve, R. J. H., and Wolters, H. B. M., *Z. Anorg. Allg. Chem.* **376,** 165 (1970).
7. Ratnasamy, P., Rodrique, L., and Leonard, A., *J. Phys. Chem.* **77,** 2242 (1973).
8. Stevens, G. C., and Edmonds, T., *J. Catal.* **37,** 544 (1975).
9. Diemann, E., *Z. Anorg. Allg. Chem.* **432,** 127 (1977).
10. Liang, K. S., deNeufville, J. P., Jacobson, A. J., Chianelli, R. R., and Betts, F., *J. Non-cryst. Solids 35* and *36,* II, 1249 (1980).
11. Liang, K. S., Cramer, S. P., Johnston, D. C., Chang, C. H., Jacobson, A. J., deNeufville, J. P., and Chianelli, R. R., *J. Non-cryst. Solids,* **42,** 345 (1980).
12. Lannin, J. S., *in* "Proceedings, 7th Intern. Conf. Amorphous and Liquid Semiconductors" (W. E. Spear, Ed.), p. 110. University of Edinburgh, 1977.
13. Stevens, G. C., and Edmonds, T., *J. Catal.* **44,** 488 (1976).
14. Muller, A., and Diemann, E., *Z. Naturforsch. B* **23,** 1607 (1968).
15. Verble, J. L., and Wieting, T. J., *Phys. Rev. Lett.* **25,** 362 (1970).
16. Wieting, T. J., and Verble, J. L., *Phys. Rev. B* **3,** 4286 (1971).
17. Meyer, B., *Chem. Rev.* **76,** 367 (1976).
18. Ratnasamy, P., and Leonard, A. J., *J. Catal.* **26,** 352 (1972).
19. Klug, H. P., and Alexander, L. E., "X-Ray Diffraction Procedures for Polycrystalline and Amorphous Materials," 2nd ed. Wiley, New York, 1974.
20. Rode, E. Ya., and Lebedev, B. A., *Russ. J. Inorg. Chem.* **6,** 608 (1961).
21. Ward, A. T., *J. Phys. Chem.* **72,** 4133 (1968).
22. Rittner, W., Muller, A., Neumann, A., Bather, W., and Sharma, R. C., *Angew. Chem. Int. Ed. Engl.* **18,** 530 (1979).
23. Muller, A., Nolte, W. O., and Krebs, B., *Angew. Chem. Int. Ed. Engl.* **17,** 279 (1978).
24. Mennemann, K., and Mattes, R., *Angew. Chem. Int. Ed. Engl.* **16,** 260 (1977).
25. Galliardt, D. W., Nieveen, W. R., and Kirby, R. D., *Solid State Commun.* **34,** 37 (1980).
26. Jandl, S., Cavellin, C. D., and Harbec, J. Y., *Solid State Comun.* **31,** 351 (1979); Harbec, J. Y., Cavellin, C. D., and Jandl, S., *Phys. Status Solidi B* **96,** K117 (1979).
27. Cavellin, C. D., and Jandl, S., *Solid State Commun.* **33,** 813 (1980).
28. Tsang, J. C., Hermann, C., and Shafer, M. W., *Conf. Ser. Inst. Phys.* **43,** 457 (1979).
29. Perrin, C., Perrin, A., and Prigent, J., *Bull. Soc. Chim. Fr.* **8,** 3086 (1972).
30. Chianelli, R. R., and Dines, M. B., *Inorg. Chem.* **14,** 2417 (1975).
31. Brattas, L., and Kjekshus, A., *Acta Chem. Scand.* **26,** 3441 (1972).
32. Jellinek, F., Pollack, R. A., and Shafer, M. W., *Mater. Res. Bull.* **9,** 845 (1974).
33. Cheng, C. P., and Schrader, G. L., *J. Catal.* **60,** 276 (1979).